Supporting Information

Trimodal hierarchical porous carbon nanorods enable high-performance Na-Se batteries

Xiang Long Huang,[1] Xiaofeng Zhang,[1] Mingjie Yi,[5] Ye Wang,[1] Shaohui Zhang,[3] Shaokun Chong,[4] Hua Kun Liu,[2] Shi Xue Dou,[2]* Zhiming Wang[1,6]*

[1] Institute of Fundamental and Frontier Sciences, University of Electronic Science and Technology of China, 610054, P. R. China

E-mail: zhmwang@uestc.edu.cn

[2] Institute for Superconducting and Electronic Materials, University of Wollongong, North Wollongong, 2500, Australia

E-mail: shi@uow.edu.au

[3] Guangdong Provincial Key Laboratory of Micro/Nano Optomechatronic Engineering, College of Mechatronics and Control Engineering, Shenzhen University, Shenzhen 518060, P. R. China

[4] Frontiers Science Center for Flexible Electronics, Xi'an Institute of Flexible Electronics and Xi'an Institute of Biomedical Materials & Engineering, Northwestern Polytechnical University, Xi'an 710072, P. R China

[5] State Key Laboratory of Advanced Welding and Joining, Harbin Institute of Technology, Shenzhen 518055, China.

[6] Institute for Advanced Study, Chengdu University, Chengdu 610106, P. R. China

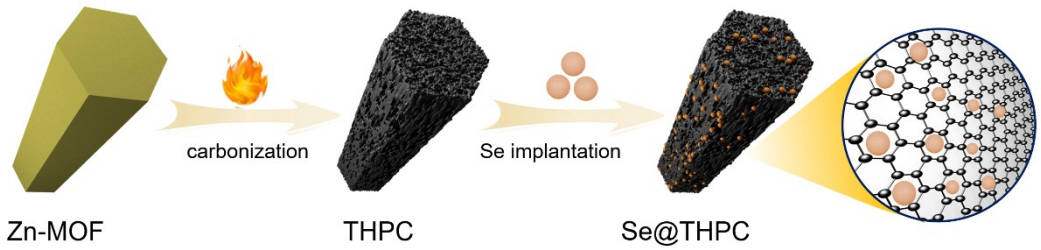

Figure S1. Schematic illustration of synthesis of the Se@THPC composite.

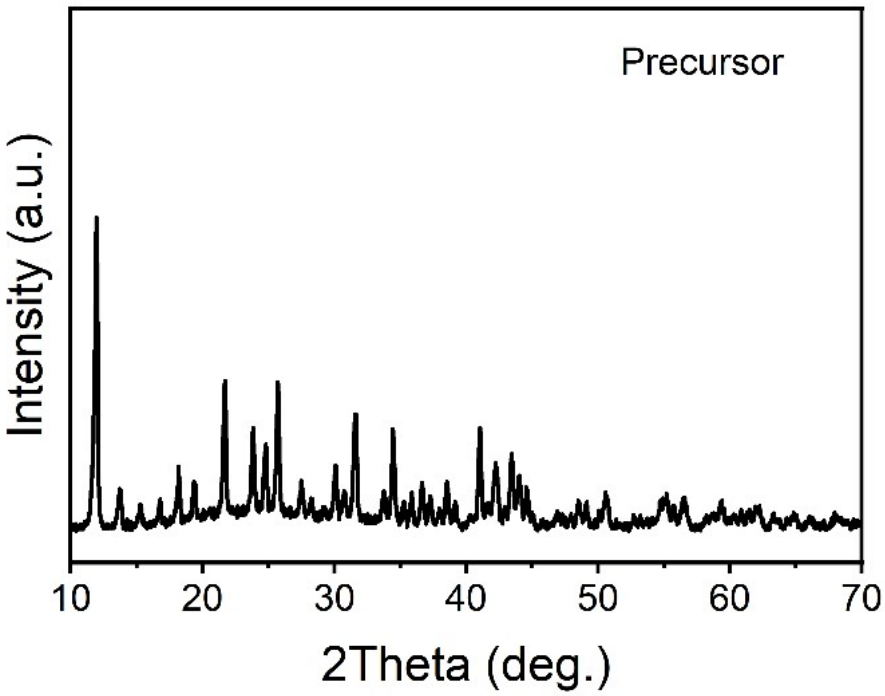

Figure S2. XRD Patterns of the Zn-MOF precursor.

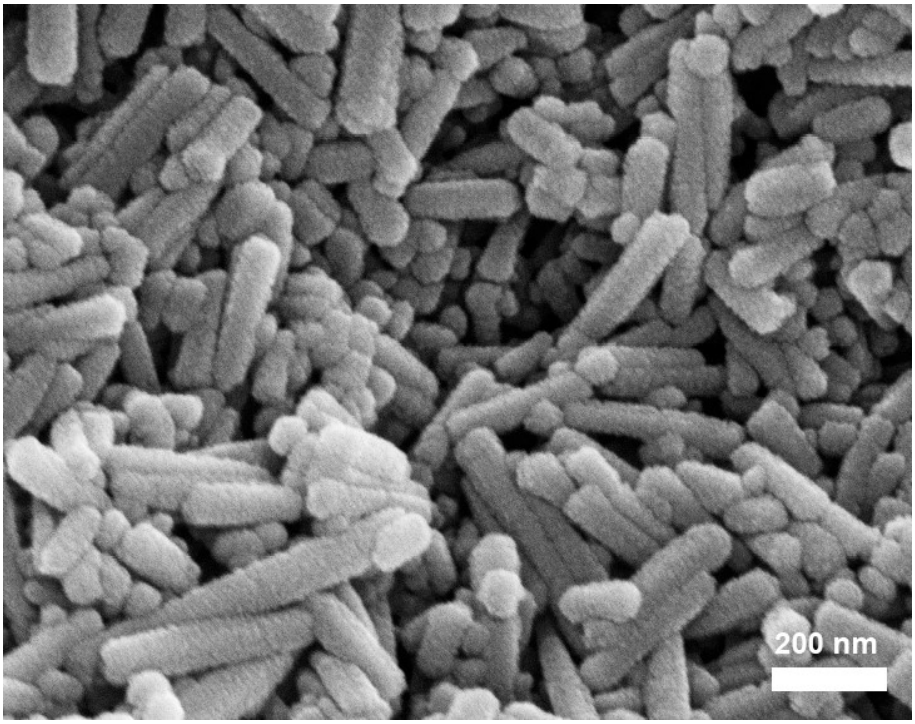

Figure S3. FESEM image of the Zn-MOF precursor.

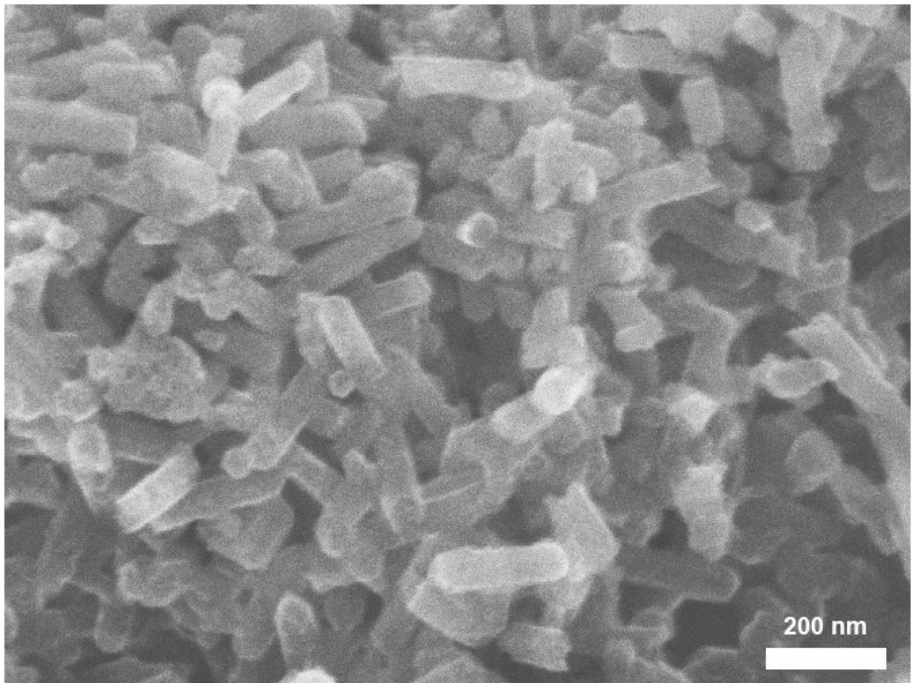

Figure S4. FESEM image of the THPC.

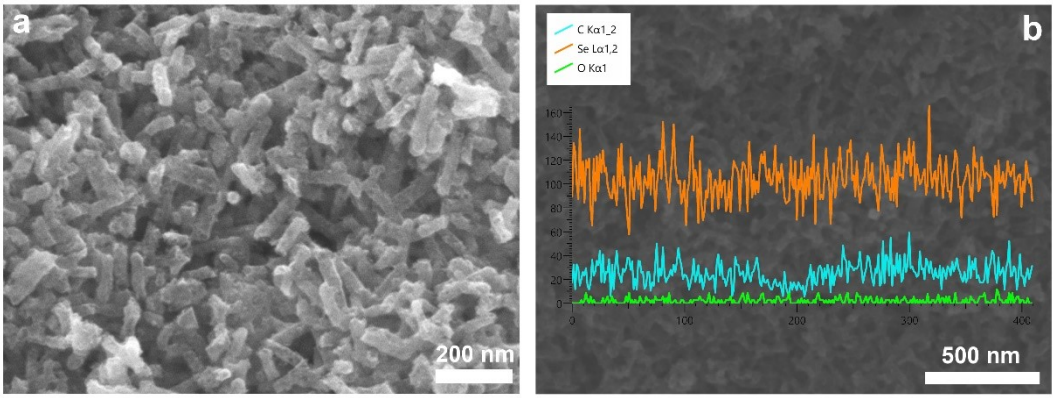

Figure S5. (a) FESEM image and linear scan (b) of the Se@THPC composite.

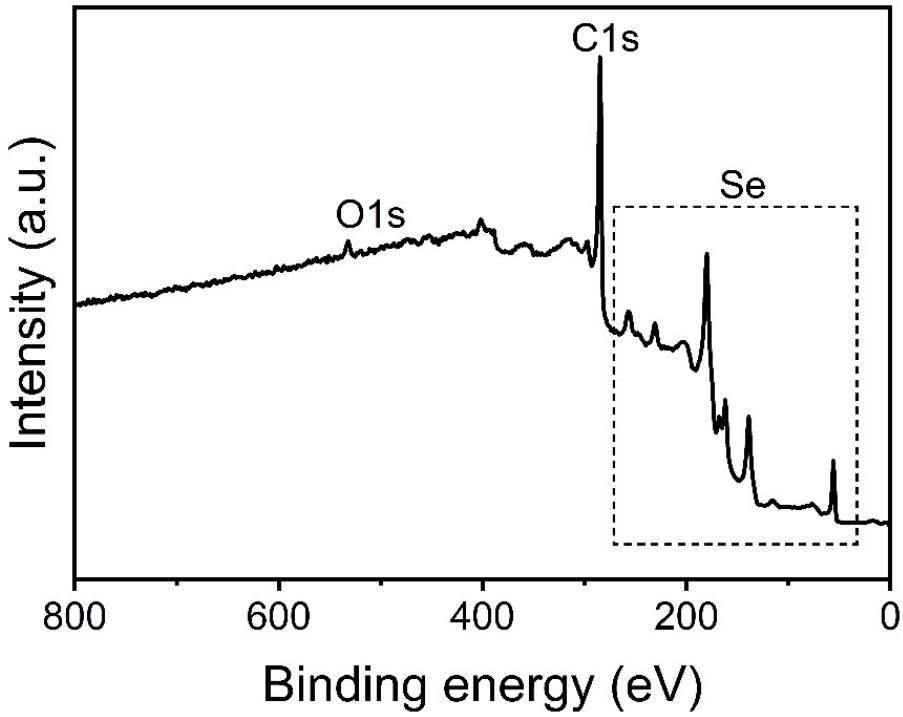

Figure 6. XPS spectra of the Se@THPC composite.

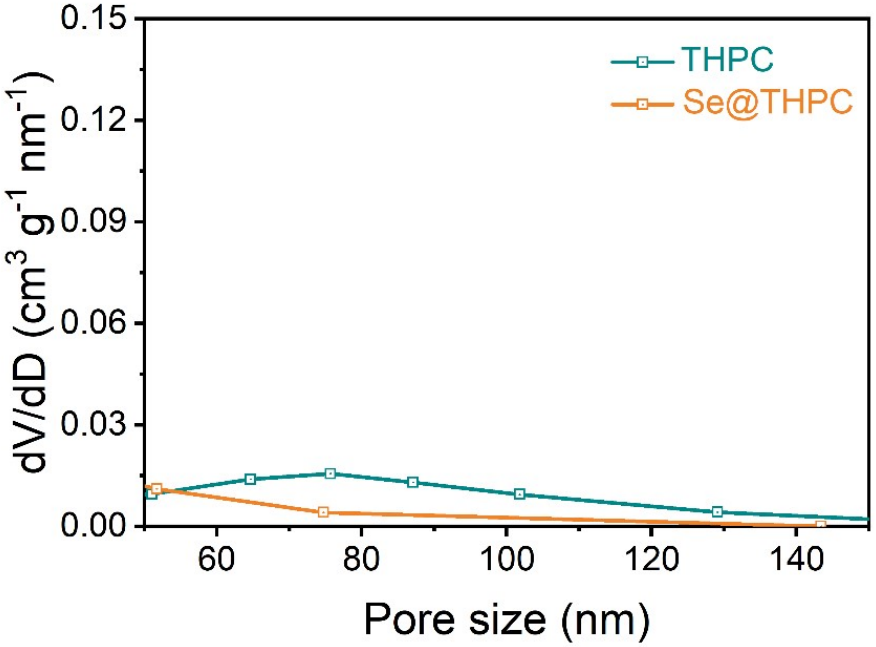

Figure S7. Pore distribution of the THPC and Se@THPC composite at a range from 50 to 150 nm.

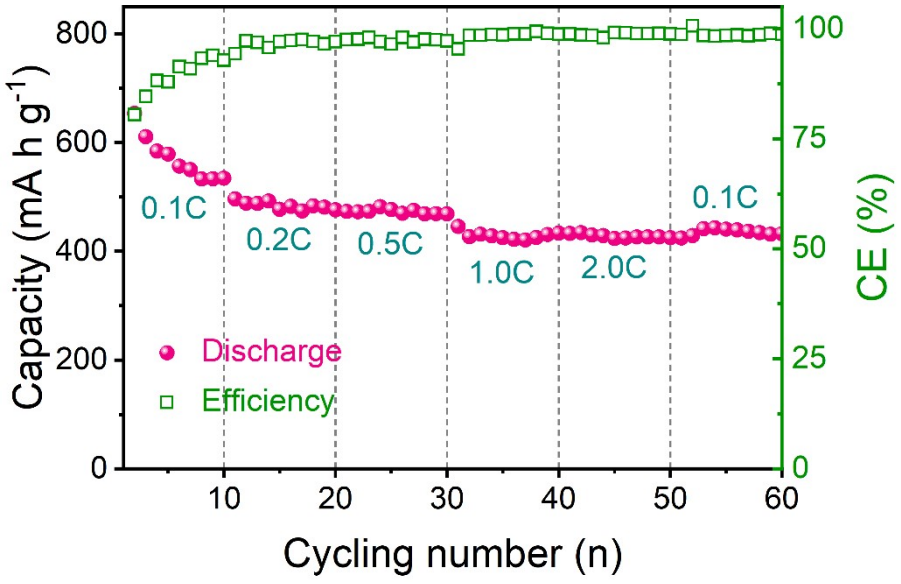

Figure S8. Rate performance of the Se@THPC composite at various rates.

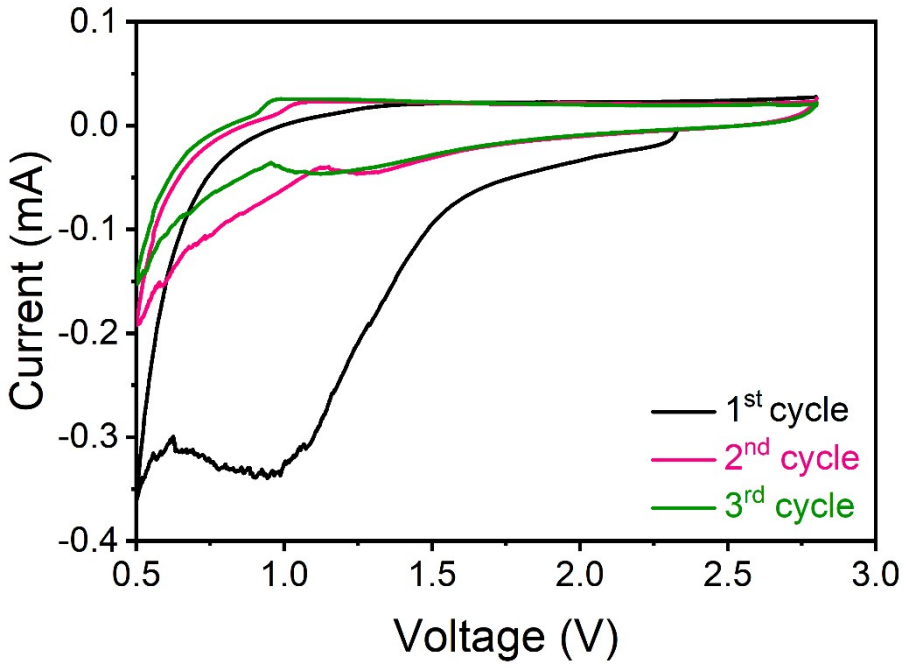

Figure S9. CV curves of the THPC at 0.1 mV s^{-1}.

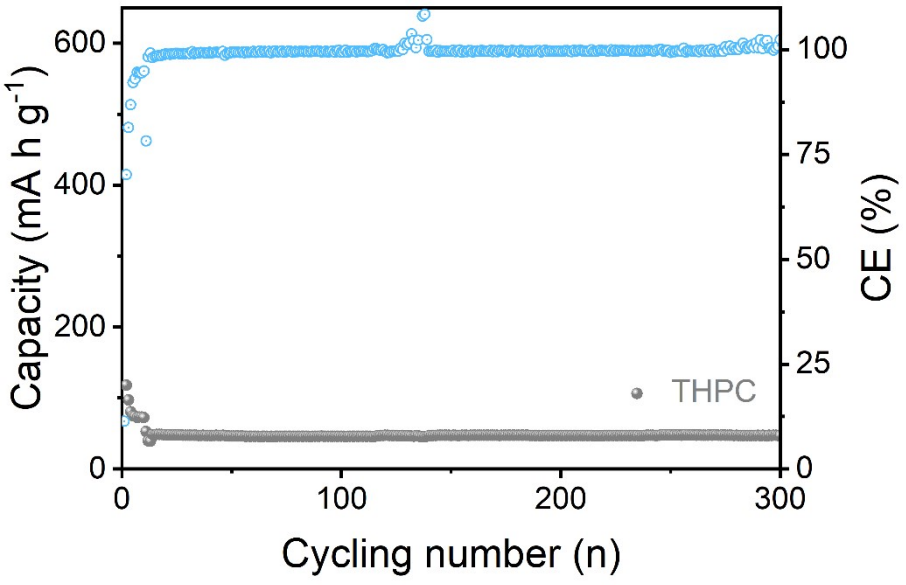

Figure S10. Cycling performance of the THPC at 675 mA g^{-1}.

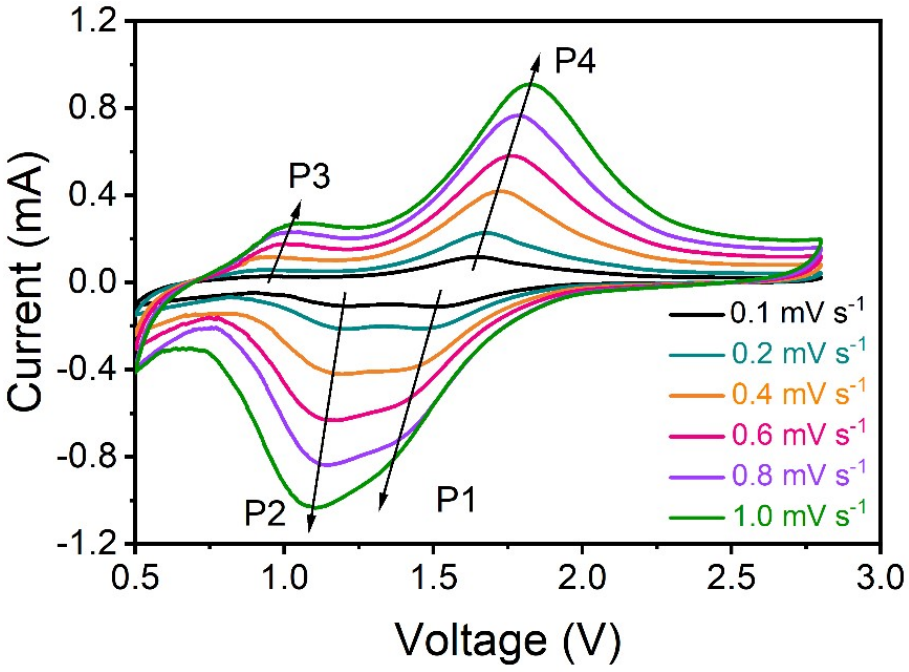

Figure S11. CV curves at a various scan rate from 0.1 to 1.0 mV s-1.

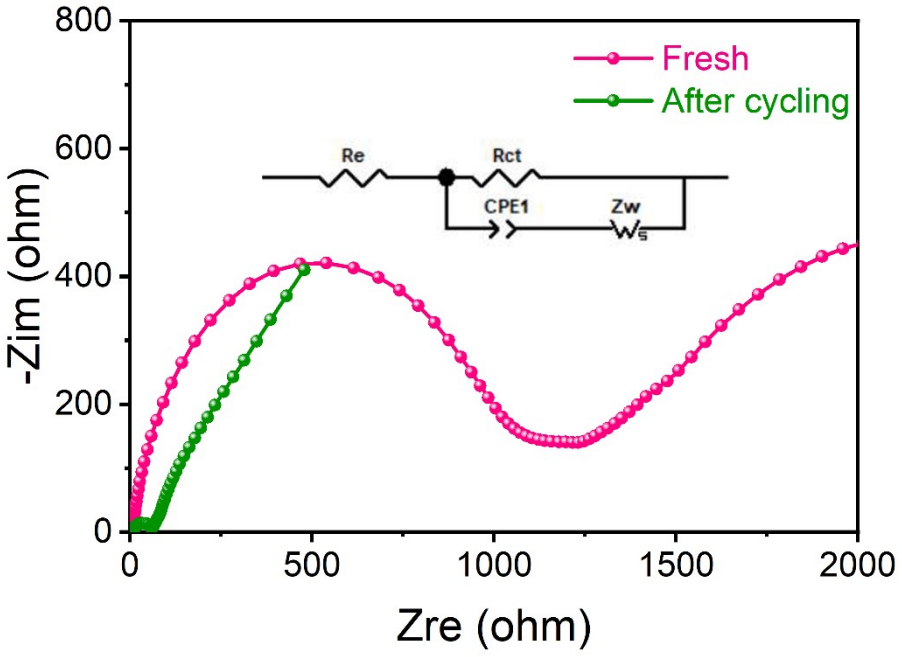

Figure S12. EIS spectra of the Se@THPC composite before and after cycling.

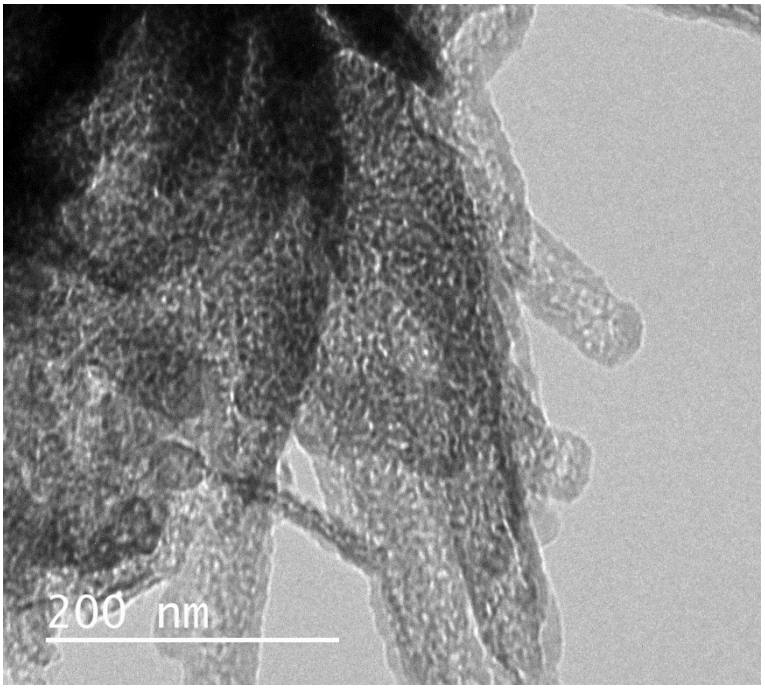

Figure S13. TEM image of the Se@THPC composite after cycling.

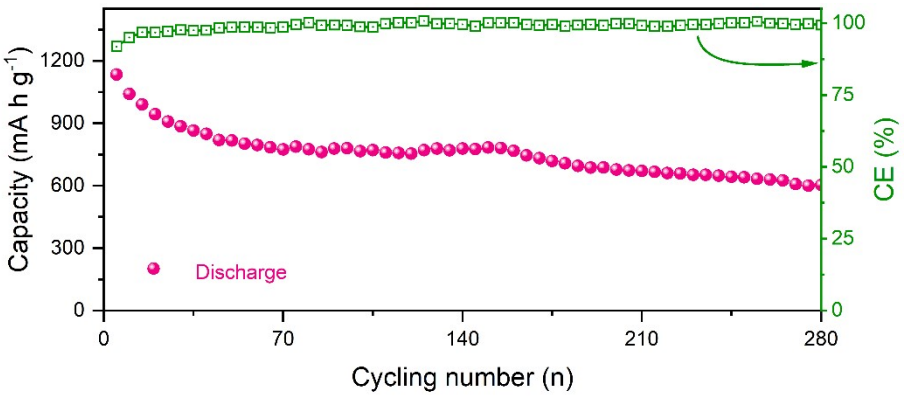

Figure S15. Cycling performance of the SeS_2@THPC composite at 0.2 A g^{-1}.

Refences involved in Figure 4d:

1. Xu, Q.; Liu, T.; Li, Y.; Hu, L.; Dai, C.; Zhang, Y.; Li, Y.; Liu, D.; Xu, M., Selenium Encapsulated into Metal–Organic Frameworks Derived N-Doped Porous Carbon Polyhedrons as Cathode for Na–Se Batteries. ACS Applied Materials & Interfaces 2017, 9 (47), 41339-41346.

2. Xu, Q.; Liu, H.; Du, W.; Zhan, R.; Hu, L.; Bao, S.; Dai, C.; Liu, F.; Xu, M., Metal-organic complex derived hierarchical porous carbon as host matrix for rechargeable Na-Se batteries. Electrochimica Acta 2018, 276, 21-27.

3. Xiao, F.; Yang, X.; Yao, T.; Wang, H.; Rogach, A. L., Encapsulation of selenium in MOF-derived N, O-codoped porous flower-like carbon host for Na-Se batteries. Chemical Engineering Journal 2022, 430, 132737.

4. Sun, W.; Guo, K.; Fan, J.; Min, Y.; Xu, Q., Confined Selenium in N-Doped Mesoporous Carbon Nanospheres for Sodium-Ion Batteries. ACS Applied Materials & Interfaces 2021, 13 (14), 16558-16566.

5. Ding, J., Zhou, H., Zhang, H., Tong, L., Mitlin, D., Selenium Impregnated Monolithic Carbons as Free-Standing Cathodes for High Volumetric Energy Lithium and Sodium Metal Batteries. Adv. Energy Mater. 2018, 8, 1701918.

6. Dong, W.; Chen, H.; Xia, F.; Yu, W.; Song, J.; Wu, S.; Deng, Z.; Hu, Z.-Y.; Hasan, T.; Li, Y.; Wang, H.; Chen, L.; Su, B.-L., Selenium clusters in Zn-glutamate MOF derived nitrogen-doped hierarchically radial-structured microporous carbon for advanced rechargeable Na–Se batteries. Journal of Materials Chemistry A 2018, 6 (45), 22790-22797.